



## RESEARCH ARTICLE

[View Article Online](#)  
[View Journal](#) | [View Issue](#)

 Cite this: *Inorg. Chem. Front.*, 2022, **9**, 5032

# Na<sub>3</sub>B<sub>6</sub>O<sub>10</sub>(HCOO): an ultraviolet nonlinear optical sodium borate-formate†

 Yi-Nan Zhang,<sup>a</sup> Qing-Fen Li,<sup>a</sup> Bing-Ben Chen,<sup>a</sup> You-Zhao Lan,<sup>a</sup>  
 Jian-Wen Cheng \*<sup>a</sup> and Guo-Yu Yang \*<sup>b</sup>

A new sodium borate-formate, Na<sub>3</sub>B<sub>6</sub>O<sub>10</sub>(HCOO) (**1**), has been successfully synthesized in a surfactant-thermal system. Compound **1** crystallizes in the orthorhombic system, with the polar *P2<sub>1</sub>2<sub>1</sub>2<sub>1</sub>* space group and the parameters *a* = 7.6375(8) Å, *b* = 9.9345(9) Å, *c* = 12.7231(13) Å, *V* = 965.36(17) Å<sup>3</sup>, and *Z* = 4. Compound **1** contains basic building units of (B<sub>6</sub>O<sub>13</sub>)<sup>8-</sup>, and each (B<sub>6</sub>O<sub>13</sub>)<sup>8-</sup> unit connects with six other neighboring units and forms a novel 3D open-framework with 9R channels. The channels accommodate Na<sup>+</sup> ions and HCOO<sup>-</sup> units. The whole framework can be simplified as a *pcu*-type net. Compound **1** shows a moderate second-harmonic-generation (SHG) signal, a short cut-off edge in the ultraviolet (UV) region, and a suitable birefringence of 0.062 at 1064 nm. These characteristics reveal that compound **1** is a promising UV nonlinear optical crystal. Density functional theory calculations show that the B–O and HCOO<sup>-</sup> units are responsible for the nonlinear optical properties of **1**.

 Received 30th June 2022,  
 Accepted 8th August 2022

DOI: 10.1039/d2qi01410f

[rsc.li/frontiers-inorganic](http://rsc.li/frontiers-inorganic)

## Introduction

Ultraviolet (UV) and deep-UV nonlinear optical (NLO) materials can generate coherent UV and deep UV light through solid-state lasers, and are widely used in photolithography and semiconductor manufacturing.<sup>1–10</sup> In a comprehensive viewpoint, Halasyamani and co-workers summarized the features of a perfect UV and deep-UV NLO material: a wide transparency region, large second-harmonic generation (SHG) coefficients, moderate birefringence, large laser damage threshold, chemical stability, and easy growth of large high-quality single crystals.<sup>11</sup> Alkali- and alkaline-earth-metal borates are important sources of UV NLO materials. β-BaB<sub>2</sub>O<sub>4</sub> (BBO), LiB<sub>3</sub>O<sub>5</sub> (LBO), and CsLiB<sub>6</sub>O<sub>10</sub> (CLBO) are commercial products, and are known as excellent UV NLO materials.<sup>12</sup> The combination of borates with other selected anions in one acentric structure may improve their NLO properties. In KBe<sub>2</sub>BO<sub>3</sub>F<sub>2</sub> (KBBF) containing [(BeO<sub>3</sub>F)(BO<sub>3</sub>)] layers and separated K<sup>+</sup> ions, blue-shifted cutoff edges have been observed due to the high electronegativity of fluorine ions, and KBBF can generate

coherent deep-UV radiation at 177.3 nm through frequency conversion.<sup>13</sup> The groups of Pan and Ye further developed the fluorooxoborate system,<sup>14,15</sup> where NH<sub>4</sub>B<sub>4</sub>O<sub>6</sub>F is impressive with an enhanced SHG efficiency (2.5KBBF). NH<sub>4</sub>B<sub>4</sub>O<sub>6</sub>F does not contain toxic beryllium ions and bulk crystals can be easily grown.<sup>14a</sup>

CO<sub>3</sub><sup>2-</sup> shows a similar planar triangle structure to BO<sub>3</sub><sup>3-</sup>, and the incorporation of CO<sub>3</sub><sup>2-</sup> into borates gives a new family of borate-carbonates.<sup>16</sup> NaRb<sub>3</sub>B<sub>6</sub>O<sub>9</sub>(OH)<sub>3</sub>(HCO<sub>3</sub>) contains isolated HCO<sub>3</sub><sup>-</sup> groups and [B<sub>6</sub>O<sub>9</sub>(OH)<sub>3</sub>]<sup>3-</sup> chains and exhibits a transparency of about 40% at 200 nm and a moderate SHG response (0.5KDP).<sup>17</sup> Borate-iodates are also known,<sup>18</sup> with Be<sub>2</sub>(BO<sub>3</sub>)(IO<sub>3</sub>) featuring a typical KBBF structure, in which honeycomb Be<sub>2</sub>BO<sub>5</sub> layers are linked by IO<sub>3</sub><sup>-</sup> groups, and shows a large birefringence ( $\Delta n = 0.172$ ) and a very strong SHG response (7.2KDP) due to the introduction of trigonal-pyramidal IO<sub>3</sub><sup>-</sup> anions.<sup>18a</sup> The introduction of tetrahedral SiO<sub>4</sub><sup>4-</sup>, GeO<sub>4</sub><sup>4-</sup>, and PO<sub>4</sub><sup>3-</sup> groups is also reported.<sup>19–21</sup> For example, Cs<sub>2</sub>GeB<sub>4</sub>O<sub>9</sub> consisting of corner-sharing B<sub>4</sub>O<sub>9</sub> and GeO<sub>4</sub> tetrahedra, is a new UV NLO crystal with a strong SHG response (2.8KDP) and large crystal dimensions of about 20 × 16 × 8 mm<sup>3</sup> grown by a high-temperature top-seeded solution method.<sup>20a</sup> In addition, with judicious selection of stereochemically active lone pair cations, a stronger SHG response is possible. Bi<sub>3</sub>TeBO<sub>9</sub> (20KDP), Pb<sub>2</sub>B<sub>5</sub>O<sub>9</sub>I (13.5KDP), Pb<sub>2</sub>BO<sub>3</sub>I (10KDP), and Pb<sub>2</sub>(BO<sub>3</sub>)(NO<sub>3</sub>) (9KDP) are notable examples,<sup>22–25</sup> in which Pb<sub>2</sub>BO<sub>3</sub>I has the highest SHG response in the KBBF family. However, these NLO crystals are not suitable for use in the UV and deep-UV regions due to their red-shifted absorption edges.<sup>24</sup>

<sup>a</sup>Key Laboratory of the Ministry of Education for Advanced Catalysis Materials, Institute of Physical Chemistry, Zhejiang Normal University, Jinhua, Zhejiang 321004, China. E-mail: jwcheng@zjnu.cn

<sup>b</sup>MOE Key Laboratory of Cluster Science, School of Chemistry and Chemical Engineering, Beijing Institute of Technology, Beijing 100081, China. E-mail: ygy@bit.edu.cn

† Electronic supplementary information (ESI) available: Additional characterization data. CCDC 2179766. For ESI and crystallographic data in CIF or other electronic format see DOI: <https://doi.org/10.1039/d2qi01410f>

Alkali- and alkaline-earth-metal formates are known as UV NLO crystals. For example, the output of UV light at around 243 nm with 1.4 mW of power has been achieved using frequency conversion with a HCOOLi-H<sub>2</sub>O single crystal, and a theoretical calculation further indicates that HCOO<sup>-</sup> dominates the contribution to the SHG efficiency.<sup>26,27</sup> Recently, Huang, Zou, and co-workers investigated the borate-formate system, and synthesized Na(HCOO)(H<sub>3</sub>BO<sub>3</sub>)(H<sub>2</sub>O)<sub>2</sub>, (HCOOH)<sub>3</sub>(H<sub>3</sub>BO<sub>3</sub>)<sub>2</sub>·3H<sub>2</sub>O, and M<sub>3</sub>(HCOO)<sub>3</sub>(H<sub>3</sub>BO<sub>3</sub>)<sub>2</sub> (M = K, Rb, Cs, NH<sub>4</sub>).<sup>28,29</sup> (NH<sub>4</sub>)<sub>3</sub>(HCOO)<sub>3</sub>(H<sub>3</sub>BO<sub>3</sub>)<sub>2</sub> shows graphite-like layers *via* the linkage of hydrogen bonding, and this compound is a UV NLO crystal with a large birefringence of 0.156 at 546 nm.<sup>29</sup> Note that all of these borate-formates contain isolated H<sub>3</sub>BO<sub>3</sub> molecules, and short UV absorption edges are found in these compounds. It is interesting to continue synthesizing UV NLO materials in the borate-formate system; other crystalline phases with different polyborate anions may be obtained.

In recent years, we obtained a new family of UV and deep-UV NLO alkali- and alkaline-earth-metal borates,<sup>30–32</sup> including LiBa<sub>3</sub>(OH)[B<sub>9</sub>O<sub>16</sub>][B(OH)<sub>4</sub>], Li<sub>2</sub>CsB<sub>7</sub>O<sub>10</sub>(OH)<sub>4</sub>, and Ba<sub>2</sub>B<sub>10</sub>O<sub>16</sub>(OH)<sub>2</sub>·(H<sub>3</sub>BO<sub>3</sub>)(H<sub>2</sub>O). Ba<sub>2</sub>B<sub>10</sub>O<sub>16</sub>(OH)<sub>2</sub>·(H<sub>3</sub>BO<sub>3</sub>)(H<sub>2</sub>O) exhibits a layered structure with two different boron oxide units of H<sub>3</sub>BO<sub>3</sub> mole-

cules and [B<sub>5</sub>O<sub>10</sub>(OH)]<sup>6-</sup> anions, and this barium borate is a possible deep-UV nonlinear-optical material.<sup>32</sup> In this work, we obtained a new sodium borate-formate, Na<sub>3</sub>B<sub>6</sub>O<sub>10</sub>(HCOO) (1), which contains both borate and formate anionic groups, and displays a 3D open-framework structure with a primitive cubic net. Compound 1 is a potential UV NLO crystal owing to its moderate SHG signal intensity, short UV cutoff edge, and suitable birefringence of 0.062 at 1064 nm.

## Methods

### Calculation method

The electronic band structure of 1 was calculated by the local density approximation (LDA) combined with the pseudopotential plane wave method implemented in the CASTEP code of Material Studio 4.0.<sup>33</sup> The cutoff energy of the plane wave base was set to 750 eV. The Monkhorst-Pack *k*-point sampling was set to the *k*-point separation of 0.005 Å<sup>-1</sup> (equivalent to 26 × 20 × 16) and 0.015 Å<sup>-1</sup> for calculating the electronic band structure and the density of states, respectively. The optical properties of 1 were determined using the sum-over-states (SOS) method implemented in our SOS program.<sup>34,35</sup> The

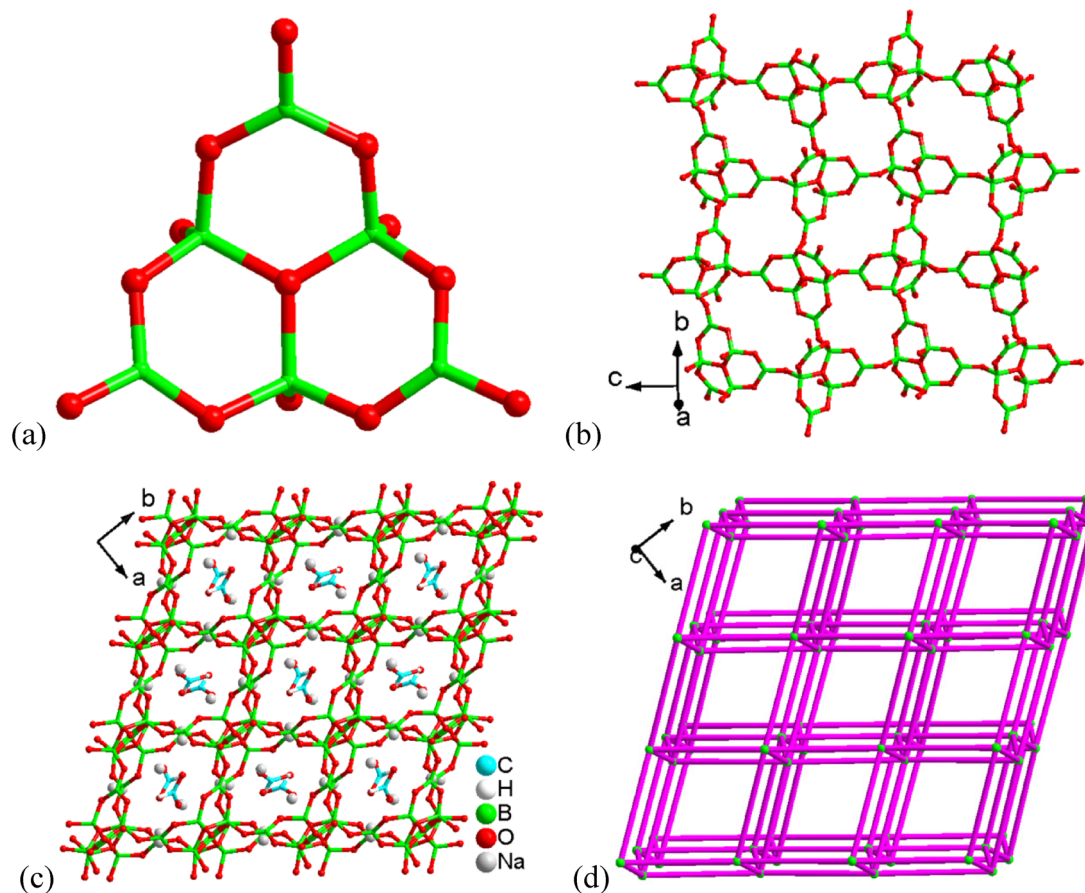


**Fig. 1** (a) (B<sub>6</sub>O<sub>13</sub>)<sup>8-</sup> cluster in 1. (b) View of the layer in 1 along the *a*-axis. (c) Framework structure of 1 viewed along the *c*-axis, with Na<sup>+</sup> and HCOO<sup>-</sup> ions occupying the channels. (d) The simplified pcu-type net in 1, in which the (B<sub>6</sub>O<sub>13</sub>)<sup>8-</sup> clusters are shown as green nodes.

Monkhorst–Pack  $k$ -point sampling of  $0.01 \text{ \AA}^{-1}$  (equivalent to  $13 \times 10 \times 8$ ) and 200 empty bands were used in the SOS calculations.

### Experimental method

Synthesis of **1**. A mixture of HCOONa (1 mmol, 0.068 g), 0.25 mL NaOH ( $4 \text{ mol L}^{-1}$ ), 333  $\mu\text{L}$  trimethyl borate, 1 mL formamide and 4 mL PEG-400 was sealed in a 30 mL Teflon-lined bomb at  $180 \text{ }^\circ\text{C}$  for 6 days, and then cooled to room temperature. Colorless lamellar crystals of **1** were obtained by filtration, which were washed with distilled water, and dried in air (15% yield based on  $\text{HCOO}^-$ ). IR (KBr,  $\text{cm}^{-1}$ ): 3433(s), 2974(w), 2779(w), 2697(m), 1626(s), 1349(s), 1172(m), 1072(w), 1022(s), 902(w), 851(w), 744(w), 694(w), 625(w), 599(w), 524(w) (Fig. S1†).

## Results and discussion

Colorless crystals of **1** were synthesized through surfactant-thermal reactions of HCOONa, NaOH, trimethyl borate, and formamide in poly(ethylene glycol)-400 at  $180 \text{ }^\circ\text{C}$  for 6 days (see the Experimental section). It should be stressed that compound **1** could not be obtained when inorganic  $\text{H}_3\text{BO}_3$  was used as the B source under similar conditions. The powder

X-ray diffraction (PXRD) patterns indicate the phase purity of **1** (Fig. S2†). Compound **1** crystallizes in the orthorhombic polar space group  $P2_12_12_1$  (Table S1†).<sup>36</sup> In the asymmetric unit of **1**, there are one unique  $\text{B}_6\text{O}_{10}$  unit, one unique  $\text{HCOO}^-$ , and three Na ions (Fig. S3†). The calculated bond-valence-sums of B, Na, and O atoms are consistent with their valences of  $3+$ ,  $1+$ , and  $2-$ , respectively. The B atoms show two coordination modes of  $\text{BO}_4$  tetrahedra (B2, B3, B5) and  $\text{BO}_3$  triangles (B1, B4, B6). The basic building unit of  $(\text{B}_6\text{O}_{13})^{8-}$  contains three 3-rings (3R), and consist of three  $\text{BO}_4$  tetrahedra (T) and three  $\text{BO}_3$  triangles ( $\Delta$ ), which are connected by corner-sharing oxygen atoms (Fig. 1a). The symbol of the  $(\text{B}_6\text{O}_{13})^{8-}$  unit can be written as  $(6 : 3\Delta + 3T)$ . The B–O bond distances vary from 1.349(4) to 1.378(4)  $\text{\AA}$  for the  $\text{BO}_3$  triangles and from 1.429(4) to 1.529(3)  $\text{\AA}$  for the  $\text{BO}_4$  tetrahedra. The Na–O bond lengths vary from 2.313(4) to 2.845(3)  $\text{\AA}$ , while the C–O bond lengths in  $\text{HCOO}^-$  are 1.214(4) and 1.237(5)  $\text{\AA}$ , respectively (Table S2†). These bond lengths are in good agreement with the reported borates and borate-formates.<sup>37,38</sup> A 3D structure is finally formed showing a primitive cubic (pcu) net, in which each  $(\text{B}_6\text{O}_{13})^{8-}$  unit connects with six other adjacent units (Fig. S4†). 9R pores are found in the  $[001]$  direction.  $\text{Na}^+$  and isolated  $\text{HCOO}^-$  units are filled in the spaces of the pores (Fig. 1b, c, d and S5†).

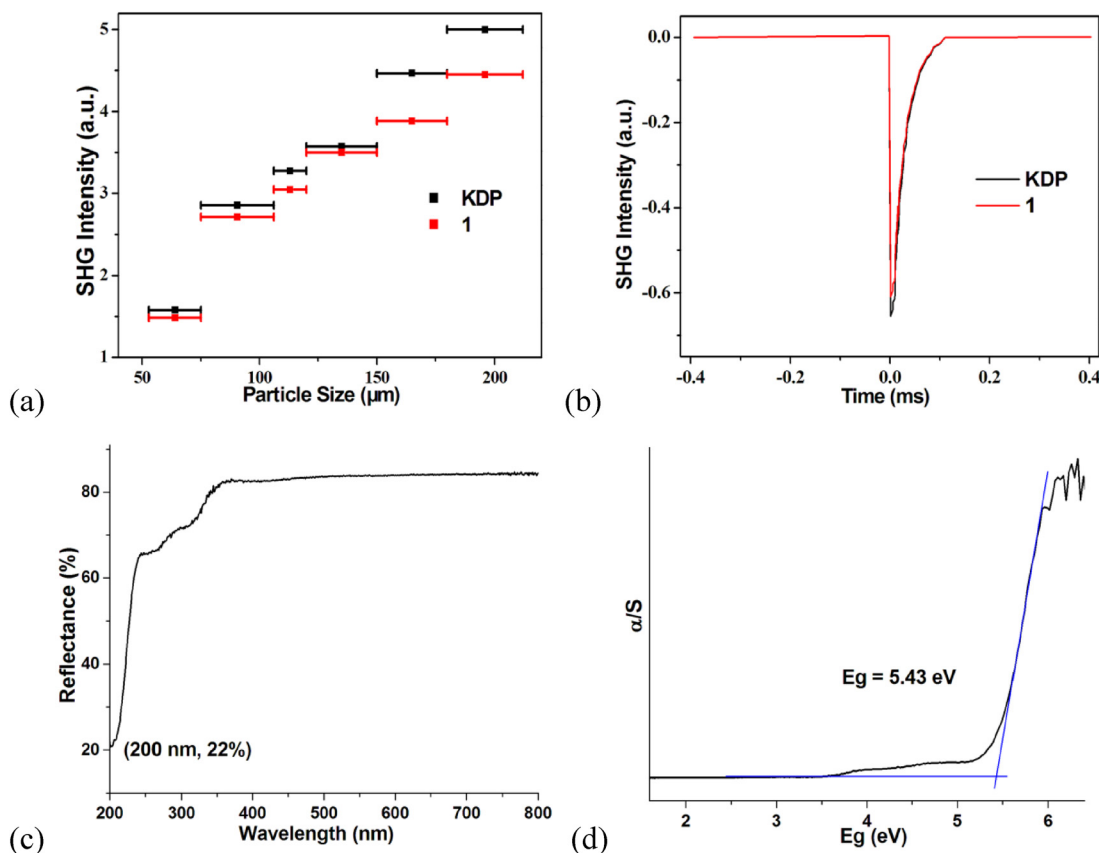
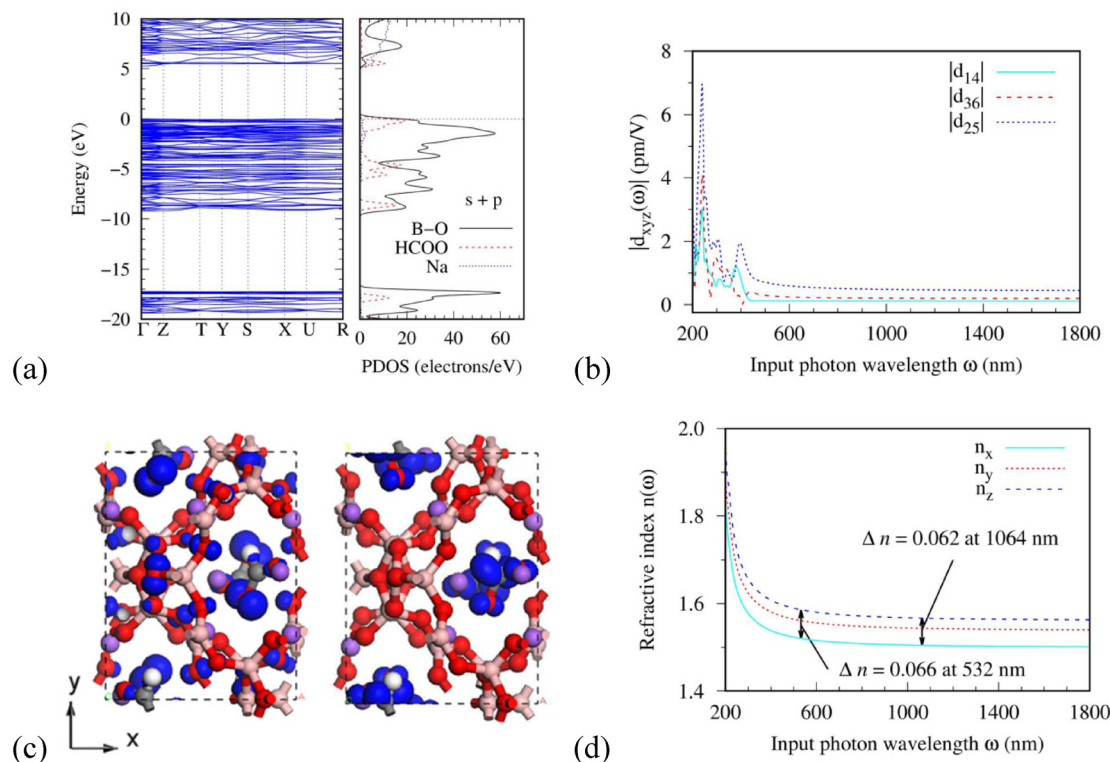


Fig. 2 (a) Phase-matching curves for **1** and KDP. (b) The SHG signals of **1** and KDP. (c) UV-vis diffuse-reflectance spectrum of **1**. (d) The band gap of compound **1**.

We performed powder SHG measurements on a Q-switched Nd:YAG laser at 1064 nm for its polar space group  $P2_12_12_1$ . The SHG signal intensity of **1** is moderate and comparable to the KDP (0.93KDP). Furthermore, compound **1** is phase-matchable as its SHG signal intensity gradually increased with larger particle size (Fig. 2a and b). The UV-vis diffuse-reflectance spectrum shows that compound **1** has a large transmission in the UV-vis region and a transparency of about 22% at 200 nm. The band gap is 5.43 eV as calculated by the Kubelka–Munk function, which corresponds to a UV cutoff edge at about 228 nm (Fig. 2c and d). These features suggest that compound **1** is a potential NLO crystal in the UV region.

To theoretically understand the optical properties of **1**, we performed first-principles density functional theory (DFT) calculations.<sup>39</sup> Fig. 3a shows the electronic band structure and the partial density of states (PDOS) for **1**. As shown in Fig. 3a, **1** is a direct-gap crystal with both the valence band maximum (VBM) and the conduction band minimum (CBM) at the  $\Gamma$  point. The theoretical band gap is 5.25 eV, which is slightly less than the experimental band gap of 5.43 eV (Fig. 2d). The difference in the band gap is due to the well-known underestimation of the energy band gap in the LDA calculation. To match the experimental band gap, the scissor correction of 0.18 eV was used in the optical calculations. Fig. 3b shows the dynamic SHG coefficients of **1**. Based on the  $D_2$  symmetry, **1** has six non-zero SHG coefficients (*i.e.*,  $xyz$ ,  $xzy$ ,  $yzx$ ,  $yxz$ ,  $zxy$ ,

$zyx$ ; the description of  $x$ ,  $y$ , and  $z$  is given in Fig. 3c). With the limit of intrinsic permutation symmetry (*i.e.*,  $xyz = yxz$ ,  $yzx = yzx$ ,  $xzy = zyx$ ), the independent SHG coefficients reduce to three elements (*i.e.*,  $xyz$ ,  $yzx$ ,  $xzy$ ). As shown in Fig. 3b, in the optical region with the input photon wavelength ( $\omega$ ) larger than the visible wavelength ( $\sim 400$  nm), the SHG coefficients have no obvious dispersion, suggesting that **1** is suitable for a very long wavelength range. When the  $\omega$  is larger than 400 nm ( $\sim 3$  eV), we observe some clear resonance enhancements. In these resonance enhancements, the linear absorption possibly takes place because the band gap is 5.43 eV, and thus these should be avoided in the nonlinear optical measurements. At 1064 nm, the largest SHG coefficient  $d_{25}$  is  $0.46 \text{ pm V}^{-1}$ , which is close to  $d_{36}(\text{KDP}) \times 1.2$  and in agreement with the experimental measurement  $d_{36}(\text{KDP}) \times 0.93$ . The PDOS indicates that the B–O and  $\text{HCOO}^-$  units are responsible for the optical properties of **1**, because the electronic transitions between the VB and CB states close to the band gap generally determine the optical response;<sup>40</sup> these results are similar to our recent work.<sup>31b,32</sup> The  $\text{HCOO}^-$  units occupying only the channels contribute significantly to the states near the CB edge (Fig. 3a), suggesting that the  $\text{HCOO}^-$  units contribute significantly to the nonlinear polarization, which is consistent with previous theoretical reports.<sup>27</sup> Furthermore, the frontier orbitals (Fig. 3c) at the  $\Gamma$  point show a clear charge transfer from the B–O units to the  $\text{HCOO}^-$  units. Finally, to inspect the phase-



**Fig. 3** (a) Electronic band structure and PDOS for **1**. (b) Dynamic second harmonic generation coefficients  $|d_{xyz}|$ . (c) The highest occupied orbital (left) and the lowest unoccupied orbital (right) at the  $\Gamma$  point. Color code: B, pink; O, red; Na, purple; C, dark grey; H, white; molecular orbital, blue. (d) Calculated refractive index  $n$  for **1**.

matching conditions, we show the calculated refractive index for **1** in Fig. 3d. We focus on the refractive indices at 1064 and 532 nm because **1** is a biaxial crystal.<sup>41</sup> At 1064 nm, the three principal indices ( $n_x$ ,  $n_y$ , and  $n_z$ ) are 1.5044, 1.5435, and 1.5669, respectively, and at 532 nm, they are 1.5204, 1.5611, and 1.5861, respectively. By sorting the three principal indices into  $n_z > n_y > n_x$ , we obtain the third refractive-index condition pointed out by M. V. Hobden,<sup>41</sup> that is,  $n_x^{2\omega} < 1/2(n_x^\omega + n_y^\omega)$ ,  $n_y^{2\omega} > 1/2(n_y^\omega + n_z^\omega)$ ,  $n_z^{2\omega} > n_z^\omega > n_y^{2\omega} > n_y^\omega > n_x^{2\omega} > n_x^\omega$ , where  $n^\omega$  and  $n^{2\omega}$  indicate the refractive indices at 1064 and 532 nm, respectively. Furthermore, as shown in Fig. 3d,  $\Delta n$  is between 0.06 and 0.07 at 1064 and 532 nm, which is a suitable birefringence required for meeting the phase-matching conditions in the UV region.<sup>2,42</sup>

## Conclusions

In summary, we have synthesized a new polar sodium borate-formate under surfactant-thermal conditions. The  $(\text{B}_6\text{O}_{13})^{8-}$  cluster is observed and it connects with six other neighboring units to form a 3D anionic framework with 9R channels, with  $\text{Na}^+$  and isolated  $\text{HCOO}^-$  units being found in the channels. This polar sodium borate-formate exhibits a UV absorption edge, moderate birefringence and SHG responses, and is phase-matchable. These characteristics indicate that **1** is a potential UV NLO material. DFT calculations show that the nonlinear optical response originates from the B–O units and  $\text{HCOO}^-$  ions. Our work indicates that the alkali metal borate-formate system may be suitable for finding UV NLO materials.

## Conflicts of interest

There are no conflicts to declare.

## Acknowledgements

This work was supported by the National Natural Science Foundation of China (Grant 21975224).

## Notes and references

- (a) M. Mutailipu, K. R. Poeppelmeier and S. Pan, Borates: A Rich Source for Optical Materials, *Chem. Rev.*, 2021, **121**, 1130–1202; (b) M. Mutailipu, M. Zhang, Z. Yang and S. Pan, Targeting the Next Generation of Deep-Ultraviolet Nonlinear Optical Materials: Expanding from Borates to Borate Fluorides to Fluorooxoborates, *Acc. Chem. Res.*, 2019, **52**, 791–801; (c) Z. Yang and S. Pan, Computationally Assisted Multistage Design and Prediction Driving the Discovery of Deep-Ultraviolet Nonlinear Optical Materials, *Mater. Chem. Front.*, 2021, **5**, 3507–3523.
- T. T. Tran, H. Yu, J. M. Rondinelli, K. R. Poeppelmeier and S. Pan, Halasyamani, Deep Ultraviolet Nonlinear Optical Materials, *Chem. Mater.*, 2016, **28**, 5238–5258.
- (a) P. Gong, X. Liu, L. Kang and Z. Lin, Inorganic Planar  $\pi$ -Conjugated Groups in Nonlinear Optical Crystals: Review and Outlook, *Inorg. Chem. Front.*, 2020, **7**, 839–852; (b) L. Kang, F. Liang, X. Jiang, Z. Lin and C. Chen, First-Principles Design and Simulations Promote the Development of Nonlinear Optical Crystals, *Acc. Chem. Res.*, 2020, **53**, 209–217.
- (a) Y. Pan, S. Guo, B. Liu, H. Xue and G. Guo, Second-Order Nonlinear Optical Crystals with Mixed Anions, *Coord. Chem. Rev.*, 2018, **374**, 464–469; (b) M. A. Beckett, Recent Advances in Crystalline Hydrated Borates with Non-Metal or Transition-Metal Complex Cations, *Coord. Chem. Rev.*, 2016, **323**, 2–14.
- (a) S. Bai, D. Wang, H. Liu and Y. Wang, Recent Advances of Oxyfluorides for Nonlinear Optical Applications, *Inorg. Chem. Front.*, 2021, **8**, 1637–1654; (b) J. Chen, C. Hu, F. Kong and J. Mao, High-Performance Second-Harmonic-Generation (SHG) Materials: New Developments and New Strategies, *Acc. Chem. Res.*, 2021, **54**, 2775–2783.
- (a) G. Zou and K. M. Ok, Novel Ultraviolet (UV) Nonlinear Optical (NLO) Materials Discovered by Chemical Substitution-Oriented Design, *Chem. Sci.*, 2020, **11**, 5404–5409; (b) K. M. Ok, Toward the Rational Design of Novel Noncentrosymmetric Materials: Factors Influencing the Framework Structures, *Acc. Chem. Res.*, 2016, **49**, 2774–2785.
- (a) C. Wu, X. Jiang, L. Lin, W. Dan, Z. Lin, Z. Huang, M. G. Humphrey and C. Zhang, Strong SHG Responses in a Beryllium-Free Deep-UV-Transparent Hydroxyborate via Covalent Bond Modification, *Angew. Chem., Int. Ed.*, 2021, **60**, 27151–27157; (b) C. Wu, G. Yang, M. G. Humphrey and C. Zhang, Recent Advances in Ultraviolet and Deep-Ultraviolet Second-Order Nonlinear Optical Crystals, *Coord. Chem. Rev.*, 2018, **375**, 459–488.
- (a) S. Zhao, P. Gong, L. Bai, X. Xu, S. Zhang, Z. Sun, Z. Lin, M. Hong, C. Chen and J. Luo, Beryllium-Free  $\text{Li}_4\text{Sr}(\text{BO}_3)_2$  for Deep-Ultraviolet Nonlinear Optical Applications, *Nat. Commun.*, 2014, **5**, 4019; (b) Y. Shen, S. Zhao and J. Luo, The Role of Cations in Second-Order Nonlinear Optical Materials Based on  $\pi$ -Conjugated  $[\text{BO}_3]^{3-}$  groups, *Coord. Chem. Rev.*, 2018, **366**, 1–28.
- (a) Z. Lin and G. Yang, Oxo Boron Clusters and Their Open Frameworks, *Eur. J. Inorg. Chem.*, 2011, 3857–3867; (b) H. Huppertz, New Synthetic Discoveries via High-Pressure Solid-State Chemistry, *Chem. Commun.*, 2011, **47**, 131–140; (c) C. Jin, F. Li, B. Cheng, H. Qiu, Z. Yang, S. Pan and M. Mutailipu, Double-Modification Oriented Design of a Deep-UV Birefringent Crystal Functionalized by  $[\text{B}_{12}\text{O}_{16}\text{F}_4(\text{OH})_4]$  Clusters, *Angew. Chem., Int. Ed.*, 2022, **61**, e202203984; (d) C. Jin, H. Zeng, F. Zhang, H. Qiu, Z. Yang, M. Mutailipu and S. Pan, Guanidinium Fluorooxoborates as Efficient Metal-free Short-Wavelength Nonlinear Optical Crystals, *Chem. Mater.*, 2022, **34**, 440–450.

- 10 (a) E. L. Belokoneva and O. V. Dimitrova, Acentric Polyborate,  $\text{Li}_3[\text{B}_8\text{O}_{12}(\text{OH})_3]$ , with a New Type of Anionic Layer and Li Atoms in the Cavities, *Inorg. Chem.*, 2013, **52**, 3724–3727; (b) M. A. Silver and T. E. Albrecht-Schmitt, Evaluation of *f*-element Borate Chemistry, *Coord. Chem. Rev.*, 2016, **323**, 36–51.
- 11 P. S. Halasyamani and W. Zhang, Viewpoint: Inorganic Materials for UV and Deep-UV Nonlinear-Optical Applications, *Inorg. Chem.*, 2017, **56**, 12077–12085.
- 12 (a) C. Chen, B. Wu, A. Jiang and G. You, A New-Type Ultraviolet SHG Crystal  $\beta$ - $\text{BaB}_2\text{O}_4$ , *Sci. Sin., Ser. B*, 1985, **28**, 235–243; (b) C. Chen, Y. Wu, A. Jiang, B. Wu, G. You, R. Li and S. Lin, New Nonlinear-Optical Crystal:  $\text{LiB}_3\text{O}_5$ , *J. Opt. Soc. Am. B*, 1989, **6**, 616–621; (c) Y. Mori, I. Kuroda, S. Nakajima, T. Sasaki and S. Nakai, New Nonlinear Optical Crystal: Cesium Lithium Borate, *Appl. Phys. Lett.*, 1995, **67**, 1818–1820.
- 13 B. Wu, D. Tang, N. Ye and C. Chen, Linear and Nonlinear Optical Properties of the  $\text{KBe}_2\text{BO}_3\text{F}_2$  (KBBF) Crystal, *Opt. Mater.*, 1996, **5**, 105–109.
- 14 (a) G. Shi, Y. Wang, F. Zhang, B. Zhang, Z. Yang, X. Hou, S. Pan and K. R. Poeppelmeier, Finding the Next Deep-Ultraviolet Nonlinear Optical Material:  $\text{NH}_4\text{B}_4\text{O}_6\text{F}$ , *J. Am. Chem. Soc.*, 2017, **139**, 10645–10648; (b) M. Mutailipu and S. Pan, Emergent Deep-Ultraviolet Nonlinear Optical Candidates, *Angew. Chem., Int. Ed.*, 2020, **59**, 20302–20317.
- 15 (a) G. Peng, N. Ye, Z. Lin, L. Kang, S. Pan, M. Zhang, C. Lin, X. Long, M. Luo, Y. Chen, Y. Tang, F. Xu and T. Yan,  $\text{NH}_4\text{Be}_2\text{BO}_3\text{F}_2$  and  $\gamma$ - $\text{Be}_2\text{BO}_3\text{F}$ : Overcoming the Layering Habit in  $\text{KBe}_2\text{BO}_3\text{F}_2$  for the Next-Generation Deep-Ultraviolet Nonlinear Optical Materials, *Angew. Chem., Int. Ed.*, 2018, **57**, 8968–8972; (b) S. Wang and N. Ye,  $\text{Na}_2\text{CsBe}_6\text{B}_5\text{O}_{15}$ : An Alkaline Beryllium Borate as a Deep-UV Nonlinear Optical Crystal, *J. Am. Chem. Soc.*, 2011, **133**, 11458–11461.
- 16 L. Liu, Y. Yang, J. Huang, X. Dong, Z. Yang and S. Pan, Design and Synthesis of a Series of Novel Mixed Borate and Carbonate Halides, *Chem. – Eur. J.*, 2017, **23**, 10451–10459.
- 17 F. Ding, W. Zhang, M. L. Nisbet, W. Zhang, P. S. Halasyamani, Z. Yang, S. Pan and K. R. Poeppelmeier,  $\text{NaRb}_3\text{B}_6\text{O}_9(\text{OH})_3(\text{HCO}_3)$ : A Borate-Bicarbonate Nonlinear Optical Material, *Inorg. Chem.*, 2020, **59**, 759–766.
- 18 (a) G. Peng, C. Lin, H. Fan, K. Chen, B. Li, G. Zhang and N. Ye,  $\text{Be}_2(\text{BO}_3)(\text{IO}_3)$ : The First Anion-Mixed van der Waals Member in the  $\text{KBe}_2\text{BO}_3\text{F}_2$  Family with a Very Strong Second Harmonic Generation Response, *Angew. Chem., Int. Ed.*, 2021, **60**, 17415–17418; (b) G. Peng, C. Lin, D. Zhao, L. Cao, H. Fan, K. Chen and N. Ye,  $\text{Sr}[\text{B}(\text{OH})_4](\text{IO}_3)$  and  $\text{Li}_4\text{Sr}_5[\text{B}_{12}\text{O}_{22}(\text{OH})_4](\text{IO}_3)_2$ : Two Unprecedented Metal Borate-Iodates Showing a Subtle Balance of Enlarged Band Gap and Birefringence, *Chem. Commun.*, 2019, **55**, 11139–11142.
- 19 H. Wu, H. Yu, S. Pan, Z. Huang, Z. Yang, X. Su and K. R. Poeppelmeier,  $\text{Cs}_2\text{B}_4\text{SiO}_9$ : A Deep-Ultraviolet Nonlinear Optical Crystal, *Angew. Chem., Int. Ed.*, 2013, **52**, 3406–3410.
- 20 (a) X. Xu, C. Hu, F. Kong, J. Zhang, J. Mao and J. Sun,  $\text{Cs}_2\text{GeB}_4\text{O}_9$ : A New Second-Order Nonlinear-Optical Crystal, *Inorg. Chem.*, 2013, **52**, 5831–5837; (b) J. Zhang, F. Kong, X. Xu and J. Mao, Crystal Structures and Second-Order NLO Properties of Borogermanates, *J. Solid State Chem.*, 2012, **195**, 63–72.
- 21 H. Yu, W. Zhang, J. Young, J. M. Rondinelli and P. S. Halasyamani, Design and Synthesis of the Beryllium-Free Deep-Ultraviolet Nonlinear Optical Material  $\text{Ba}_3(\text{ZnB}_5\text{O}_{10})\text{PO}_4$ , *Adv. Mater.*, 2015, **27**, 7380–7385.
- 22 M. Xia, X. Jiang, Z. Lin and R. Li, “All-Three-in-One”: A New Bismuth-Tellurium-Borate  $\text{Bi}_3\text{TeBO}_9$  Exhibiting Strong Second Harmonic Generation Response, *J. Am. Chem. Soc.*, 2016, **138**, 14190–14193.
- 23 Y. Huang, L. Wu, X. Wu, L. Li, L. Chen and Y. Zhang,  $\text{Pb}_2\text{B}_5\text{O}_9\text{I}$ : An Iodide Borate with Strong Second Harmonic Generation, *J. Am. Chem. Soc.*, 2010, **132**, 12788–12789.
- 24 H. Yu, N. Z. Koocher, J. M. Rondinelli and P. S. Halasyamani,  $\text{Pb}_2\text{BO}_3\text{I}$ : A Borate Iodide with the Largest Second-Harmonic Generation (SHG) Response in the  $\text{KBe}_2\text{BO}_3\text{F}_2$  (KBBF) Family of Nonlinear Optical (NLO) Materials, *Angew. Chem., Int. Ed.*, 2018, **57**, 6100–6103.
- 25 J. Song, C. Hu, X. Xu, F. Kong and J. Mao, A Facile Synthetic Route to a New SHG Material with Two Types of Parallel  $\pi$ -Conjugated Planar Triangular Units, *Angew. Chem., Int. Ed.*, 2015, **54**, 3679–3682.
- 26 C. J. Foot, P. E. G. Baird, M. G. Boshier, D. N. Stacey and G. K. Woodgate, Generation of cw 243 nm Radiation and Application to Laser Spectroscopy of the Strontium Isotopes, *Opt. Commun.*, 1984, **50**, 199–204.
- 27 C. Mang, K. Wu, C. Lin, R. Sa, P. Liu and B. Zhuang, A Theoretical Study on the Second-Order Nonlinear Optical Susceptibilities of Lithium Formate Monohydrate Crystal,  $\text{HCOOLi}\cdot\text{H}_2\text{O}$ , *Opt. Mater.*, 2003, **22**, 353–359.
- 28 (a) F. He, Q. Wang, M. Liu, L. Huang, D. Gao, J. Bi and G. Zou, Hydrogen Bonding Assisted Construction of Graphite-like Deep-UV Optical Materials with Two Types of Parallel  $\pi$ -Conjugated Units, *Cryst. Growth Des.*, 2018, **18**, 4756–4765; (b) Y. Guo, D. Zhang, T. Zheng, L. Huang, D. Gao, J. Bi and G. Zou, Noncentrosymmetric  $\text{Rb}_3(\text{COOH})_3(\text{H}_3\text{BO}_3)_2$  vs Centrosymmetric  $\text{Cs}_3(\text{COOH})_3(\text{H}_3\text{BO}_3)_2$ , *Cryst. Growth Des.*, 2021, **21**, 5976–5982.
- 29 Y. Deng, L. Wang, Y. Ge, L. Huang, D. Gao, J. Bia and G. Zou,  $(\text{NH}_4)_3[\text{B}(\text{OH})_3]_2(\text{COOH})_3$ : A Graphite-like UV Nonlinear Optical Material with a Large Birefringence via Structural Optimization, *Chem. Commun.*, 2020, **56**, 9982–9985.
- 30 (a) Q. Wei, J. Cheng, C. He and G. Yang, An Acentric Calcium Borate  $\text{Ca}_2[\text{B}_5\text{O}_9](\text{OH})\cdot\text{H}_2\text{O}$ : Synthesis, Structure, and Nonlinear Optical Property, *Inorg. Chem.*, 2014, **53**, 11757–11763; (b) Q. Wei, J. Wang, C. He, J. Cheng and G. Yang, Deep-ultraviolet Nonlinear Optics in a Borate Framework with 21-ring Channels, *Chem. – Eur. J.*, 2016, **22**, 10759–10762.
- 31 (a) E. Wang, J. Huang, S. Yu, Y. Lan, J. Cheng and G. Yang, An Ultraviolet Nonlinear Optic Borate with 13-Ring

- Channels Constructed from Different Building Units, *Inorg. Chem.*, 2017, **56**, 6780–6783; (b) J. Huang, C. Jin, P. Xu, P. Gong, Z. Lin, J. Cheng and G. Y. Yang,  $\text{Li}_2\text{CsB}_7\text{O}_{10}(\text{OH})_4$ : A Deep-Ultraviolet Nonlinear-Optical Mixed-Alkaline Borate Constructed by Unusual Heptaborate Anions, *Inorg. Chem.*, 2019, **58**, 1755–1758.
- 32 W. Zhao, Y. Zhang, Y. Lan, J. Cheng and G. Yang,  $\text{Ba}_2\text{B}_{10}\text{O}_{16}(\text{OH})_2 \cdot (\text{H}_3\text{BO}_3)(\text{H}_2\text{O})$ : A Possible Deep-Ultraviolet Nonlinear-Optical Barium Borate, *Inorg. Chem.*, 2022, **61**, 4246–4250.
- 33 Accelrys, *Materials Studio Getting Started, Release 4.0*, Accelrys Software, Inc., San Diego, 2006.
- 34 (a) J. Lin, M. H. Lee, Z. P. Liu, C. T. Chen and C. J. Pickard, Mechanism for Linear and Nonlinear Optical Effects in Beta- $\text{BaB}_2\text{O}_4$  Crystals, *Phys. Rev. B: Condens. Matter Mater. Phys.*, 1999, **60**, 13380–13389; (b) Z. S. Lin, J. Lin, Z. Z. Wang, Y. C. Wu, N. Ye, C. T. Chen and R. K. Li, Theoretical Calculations and Predictions of the Nonlinear Optical Coefficients of Borate Crystals, *J. Phys.: Condens. Matter*, 2001, **13**, R369–R384; (c) C. Aversa and J. E. Sipe, Nonlinear Optical Susceptibilities of Semiconductors: Results with a Length-Gauge Analysis, *Phys. Rev. B: Condens. Matter Mater. Phys.*, 1995, **52**, 14636–14645.
- 35 Y. Z. Lan, New Understandings of Third Harmonic Generation Coefficient of Bulk Silicon: Implementation and Application of the Full ab Initio Band Structure Sum-Over-States Method, *Comput. Condens. Matter*, 2016, **8**, 22–30.
- 36 Crystal data for **1**:  $M = 338.85$ , orthorhombic,  $P2_12_12_1$ ,  $a = 7.6375(8)$  Å,  $b = 9.9345(9)$  Å,  $c = 12.7231(13)$  Å,  $V = 965.36(17)$  Å<sup>3</sup>,  $Z = 4$ ,  $D_c = 2.331$  g cm<sup>-3</sup>,  $\mu = 0.327$  mm<sup>-1</sup>, and  $S = 1.086$ . The final least-squares refinements converged at  $R_1$  ( $wR_2$ ) = 0.0432 (0.0859) and for 1743 reflections with  $I > 2\sigma(I)$ . The intensity data were collected on a Gemini A Ultra diffractometer with graphite-monochromated Mo K $\alpha$  radiation ( $\lambda = 0.71073$  Å) at room temperature. All absorption corrections were performed using the Multiscan program. The structure was solved by direct methods and refined by full-matrix least squares on  $F^2$  with the SHELXTL-97 program.
- 37 (a) J. Wang, J. Cheng, Q. Wei, H. He, B. Yang and G. Yang,  $\text{NaB}_3\text{O}_5 \cdot 0.5\text{H}_2\text{O}$  and  $\text{NH}_4\text{NaB}_6\text{O}_{10}$ : Two Cluster Open Frameworks with Chiral Quartz and Achiral Primitive Cubic Nets Constructed from Oxo Boron Cluster Building Units, *Eur. J. Inorg. Chem.*, 2014, 4079–4083; (b) S. Zhi, Y. Wang, L. Sun, J. Cheng and G. Yang, Linking 1D Transition-Metal Coordination Polymers and Different Inorganic Boron Oxides To Construct a Series of 3D Inorganic–Organic Hybrid Borates, *Inorg. Chem.*, 2018, **57**, 1350–1355; (c) R. Pan, J. Cheng, B. Yang and G. Yang,  $\text{CsB}_x\text{Ge}_{6-x}\text{O}_{12}$  ( $x=1$ ): A Zeolite Sodalite-Type Borogermanate with a High Ge/B Ratio by Partial Boron Substitution, *Inorg. Chem.*, 2017, **56**, 2371–2374.
- 38 (a) Y. Liu, R. Pan, J. Cheng, H. He, B. Yang, Q. Zhang and G. Yang, A Series of Aluminoborates Templated or Supported by Zinc–Amine Complexes, *Chem. – Eur. J.*, 2015, **21**, 15732–15739; (b) Q. Wei, C. He, L. Sun, X. An, J. Zhang and G. Yang,  $\text{Na}_2(\text{H}_2\text{en})[\text{B}_5\text{O}_8(\text{OH})]_2$  [ $\text{B}_3\text{O}_4(\text{OH})$ ]<sub>2</sub> and  $\text{Na}_3(\text{HCOO})[\text{B}_5\text{O}_8(\text{OH})]$ : Two Borates Co-Templated by Inorganic Cations and Organic Compounds, *Eur. J. Inorg. Chem.*, 2017, 4061–4067; (c) H. Tian, W. Wang, Y. Gao, T. Deng, J. Wang, Y. Feng and J. Cheng, Facile Assembly of an Unusual Lead Borate with Different Cluster Building Units via a Hydrothermal Process, *Inorg. Chem.*, 2013, **52**, 6242–6244.
- 39 (a) A. H. Reshak, Lithium Borate  $\text{Li}_3\text{B}_5\text{O}_8(\text{OH})_2$  with Large Second Harmonic Generation and a High Damage Threshold in the Deep-Ultraviolet Spectral Range, *Phys. Chem. Chem. Phys.*, 2017, **19**, 30703–30714; (b) A. H. Reshak and S. Auluck, Two Haloid Borate Crystals with Large Nonlinear Optical Response, *Phys. Chem. Chem. Phys.*, 2017, **19**, 18416–18425.
- 40 M. H. Lee, C. H. Yang and J. H. Jan, Band-Resolved Analysis of Nonlinear Optical Properties of Crystalline and Molecular Materials, *Phys. Rev. B: Condens. Matter Mater. Phys.*, 2004, **70**, 235110.
- 41 M. V. Hobden, Phase-Matched Second-Harmonic Generation in Biaxial Crystals, *J. Appl. Phys.*, 1967, **38**, 4365.
- 42 W. Zhang, H. Yu, H. Wu and P. S. Halasyamani, Phase-Matching in Nonlinear Optical Compounds: A Materials Perspective, *Chem. Mater.*, 2017, **29**, 2655–2668.